Available online at www.sciencedirect.com
ScienceDirect
Journal of Catalysis 252 (2007) 296–302
JOURNAL OF CATALYSIS
www.elsevier.com/locate/jcat

Highly visible-light active C- and V-doped TiO_2 for degradation of acetaldehyde

Xiangxin Yang [a], Chundi Cao [a], Keith Hohn [a], Larry Erickson [a], Ronaldo Maghirang [b], Dambar Hamal [c], Kenneth Klabunde [c,*]

[a] *Department of Chemical Engineering, Kansas State University, Manhattan, KS 66506, USA*
[b] *Department of Biological & Agricultural Engineering, Kansas State University, Manhattan, KS 66506, USA*
[c] *Department of Chemistry, Kansas State University, Manhattan, KS 66506, USA*

Received 25 July 2007; revised 19 September 2007; accepted 20 September 2007

Available online 30 October 2007

Abstract

C-doped and C- and V-doped TiO_2 photocatalysts were prepared by a sol–gel process. Both catalysts showed high activity for the degradation of acetaldehyde under visible irradiation (>420 nm). The co-doped TiO_2 catalysts also were highly active in the dark; 2.0% V-containing co-doped TiO_2 had the highest activity, comparable with the activity under visible light irradiation. The catalysts were characterized by X-ray powder diffraction (XRD), X-ray photoelectron spectroscopy (XPS), diffuse reflectance spectroscopy (DRS), and N_2 adsorption–desorption. The results suggest that vanadium ions were introduced both on the surface and into the bulk of TiO_2. A free electron, induced by the formation of V^{5+} in the sublayers of TiO_2 during calcination at 500 °C in air, was delocalized and promoted into the conduction band by thermal energy and further transferred to O_2, generating a superoxide radical anion ($O_2^{\bullet-}$) that is responsible for degradation of acetaldehyde in the dark. In addition to functioning as a photosensitizer that shifts the optical response of TiO_2 from the ultraviolet (UV) to the visible light region, the doped elemental carbon increased the surface area and improved the dispersion of vanadium.

Keywords: Visible light; Carbon; Vanadium; TiO_2; Photocatalyst

1. Introduction

Photocatalytic degradation and complete mineralization of toxic organic compounds in water, soil, and air in the presence of semiconductor powders have received much attention over the last two decades [1–4]. A semiconductor is characterized by a filled valence band and an empty conduction band. When it is irradiated with light of sufficient energy corresponding to or exceeding its band gap, an electron is promoted into the conduction band, leaving a hole in the valence band. The electrons and holes are good reductants and powerful oxidants, respectively, and they can initiate redox reactions on the semiconductor surface [2]. TiO_2 is considered the most promising photocatalyst due to its high efficiency, chemical stability, nontoxicity, and relative cost. However, the use of TiO_2 is impaired by its wide band gap (3.2 eV), which requires ultraviolet irradiation for photocatalytic activation ($\lambda < 387$ nm) [5–7]. UV light accounts for only about 5% of solar energy; visible light, 45% [8]. The shift of the optical response of TiO_2 from UV to the visible spectral range will have a profound positive effect on the efficient use of solar energy in photocatalytic reactions [9]. Thus, much effort has been directed toward the development of visible light-active photocatalysts.

One approach to synthesizing visible light active photocatalysts is the substitution of Ti by V, Cr, Mn, Ni, or Fe. Anpo et al. [7] modified TiO_2 catalysts by bombarding them with high-energy metal ions. The metal ion-implanted TiO_2 showed a large absorption shift toward the visible light region, and the V ion had the highest effectiveness in the red shift. Klosek and Raftery [10] synthesized V-doped, supported TiO_2 photocatalysts that were quite active using visible light (396–450 nm). Wu and Chen [11] reported that V-doped TiO_2 acquired the

* Corresponding author. Fax: +1 785 532 6666.
E-mail address: kenjk@ksu.edu (K. Klabunde).

0021-9517/$ – see front matter
doi:10.1016/j.jcat.2007.09.014

capability of absorbing visible light and showed a "red shift" in the UV–vis spectra. Recently, it was shown that the optical response of TiO_2 also could be shifted from UV to visible light by doping with nonmetal atoms, such as carbon, nitrogen, and sulfur. Joung et al. [12] synthesized N-doped TiO_2 under a stream of ammonia gas, which had a band gap of 2.95 eV. Burda et al. [5] used the direct amination of 6- to 10-nm titania particles; the $TiO_{2-x}N_x$ nanoparticles were catalytically active and absorbed well into the visible region up to 600 nm. Umebayashi et al. [13] reported band gap narrowing of TiO_2 by sulfur doping, and that sulfur atoms were incorporated as anions and substituted for oxygen sites in the lattice of TiO_2. Ohno et al. [14] prepared sulfur cation-doped TiO_2 catalysts that showed strong absorption of visible light and high activities for degradation of methylene blue in water under irradiation at wavelengths longer than 440 nm. Doping carbonate species into a TiO_2 lattice shifted the absorption edge of TiO_2 from 400 to 700 nm or more [15,16]. Carbon-containing TiO_2 photocatalyst is capable of photodegrading 4-chlorophenol with visible light [17]. The effect of transition metal and/or nonmetal atoms on the photocatalytic activity of TiO_2 also has been studied. Sun et al. [18] observed that carbon and sulfur co-doped TiO_2 showed high photodegradation of 4-chlorophenol under visible light irradiation. Zhao et al. [19] synthesized a visible-light-driven $Ni_2O_3/TiO_{2-x}B_x$ photocatalyst; the incorporation of boron atoms into TiO_2 extended the spectral response to the visible region, and the loaded Ni_2O_3 species acted as electron traps and thus facilitated the charge separation. Wei et al. [20] reported that lanthanum and nitrogen led to significant enhancement in degrading of methyl orange under visible light ($350 < \lambda < 450$ nm); the substitution of N for O was responsible for the band gap narrowing of TiO_2, and La^{3+} doping prevented the aggregation of powder in the process of preparation. Sakatani et al. [21] found that the doped La^{3+} hindered crystal growth and that the number of the paramagnetic N species seemed to control the absorption of visible light and the activity under visible light irradiation.

The sol–gel process has been widely used to synthesize TiO_2-based photocatalysts. The incorporation of active ions (dopants) in the sol during the gelation stage allows the ions to have direct interaction with TiO_2; therefore, active ions could be doped into the lattice of TiO_2, resulting in materials with special optical and catalytic properties.

In the present research, we prepared carbon and vanadium co-doped anatase TiO_2 photocatalysts by a sol–gel process using titanium isopropoxide, vanadyl acetylacetonate, urea, and thiourea as precursors. We demonstrate enhanced photocatalytic performance of the doped catalysts.

2. Experimental

2.1. Sample preparation

Titanium isopropoxide (97%, Aldrich), vanadyl acetylacetonate (98%, Aldrich), urea (99.0–100.5%, Aldrich), and thiourea (99%, Aldrich) were used as raw materials. First, 3.8 g (0.05 mol) thiourea and 3.0 g (0.05 mol) urea were dissolved in 75 mL of deionized water. While under vigorous stirring in an ice bath, desired amounts of vanadyl acetylacetonate (corresponding to 0.5, 1, 2, and 3% of vanadium) were added to the solution. Then 11 mL (0.0375 mol) of titanium isopropoxide was added dropwise. The resulting mixture was stirred for 24 h and aged for 48 h. The water was removed by drying in air at 80 °C. The dried powder was crushed and calcined at 500 °C for 2 h in air. Pure TiO_2 catalyst was obtained using a similar method without urea and thiourea. Commercial Degussa P25 TiO_2 (anatase/rutile = 75/25) with a specific surface area of 50 m^2/g and primary particle size of 20 nm were used for comparison purposes.

2.2. Characterization

XRD patterns were obtained with a Bruker D8 diffractometer, using Cu$K\alpha$ radiation (1.5406 Å) at 40 kV and 40 mA and a secondary graphite monochromator. Samples were packed into a plastic holder. The measurements were recorded in steps of 0.025° with a count time of 4 s in the 2θ range of 20–65°. Identification of the phases was done with the help of the Joint Committee on Powder Diffraction Standards (JCPDS) files.

XPS data were recorded using a Perkin–Elmer PHI 5400 electron spectrometer using acrochromatic Al$K\alpha$ radiation (1486.6 eV) with Ar^+ sputtering to remove the surface layer of the sample. All spectra were obtained under vacuum at a pressure of about 2.0×10^{-9} Torr. The XPS binding energies were measured with precision of 0.1 eV. The analyzer pass energy was set to 17.9 eV, and the contact time was 50 ms. Before the samples were tested, the spectrometer was calibrated by setting the binding energies of Au $4f_{7/2}$ and Cu $2p_{3/2}$ to 84.0 and 932.7 eV, respectively. Binding energies for the samples were normalized with respect to the position of the C 1s peak resulting from adsorbed hydrocarbon fragments.

DRS were recorded using a Cary 500 Scan UV–vis NIR spectrophotometer with an integrating sphere attachment for their diffuse reflectance in the range of 200–800 nm. All spectra were referenced to polytetrafluoroethylene.

N_2 adsorption–desorption isotherms were obtained at −196 °C using a Quantachrome NOVA 1000 series instrument. The specific surface areas were calculated according to the multipoint BET method. Before adsorption, all samples were degassed for 1 h at 150 °C under vacuum.

2.3. Degradation of acetaldehyde

A typical indoor air pollutant, acetaldehyde, was chosen as the probe molecule for evaluating the catalyst activity. The experiments were performed in a cylindrical glass air-filled static reactor (305 mL total volume) with a quartz window. The light source was an Oriel 1000-W high-pressure Hg arc lamp. The combination of a vis-NIR long-pass filter (400 nm) and colored glass filter (>420 nm) was used to eliminate ultraviolet radiation during visible light experiments. The catalyst (100 mg) was placed in a circular glass dish and mounted in the reactor. Then 100 μL of liquid acetaldehyde was introduced into the reactor,

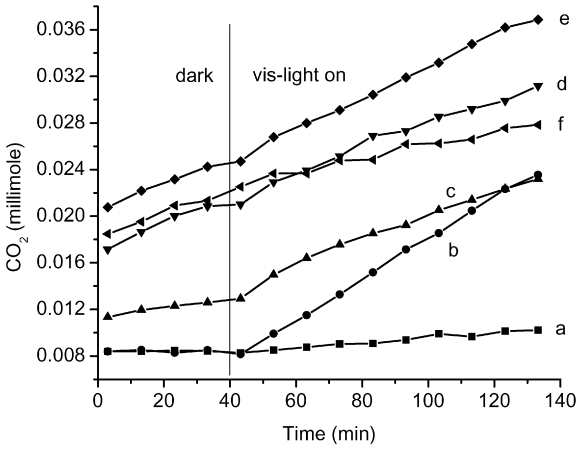

Fig. 1. CO_2 evolution during CH_3CHO oxidation on P25 TiO_2 and doped TiO_2: (a) P25 TiO_2, (b) C-doped TiO_2, (c) C-, V-doped TiO_2 (0.5% V), (d) C-, V-doped TiO_2 (1.0% V), (e) C-, V-doped TiO_2 (2% V), (f) C-, V-doped TiO_2 (3.0% V).

Table 1
Initial rate of CO_2 evolution (mmol/min)

Catalyst	In the dark	Under visible irradiation
P25 TiO_2	0	2.13×10^{-5}
C-doped TiO_2	0	1.74×10^{-4}
C-, V-doped TiO_2 (0.5% V)	3.81×10^{-5}	1.38×10^{-4}
C-, V-doped TiO_2 (1.0% V)	9.85×10^{-5}	1.40×10^{-4}
C-, V-doped TiO_2 (2.0% V)	1.26×10^{-4}	1.37×10^{-4}
C-, V-doped TiO_2 (3.0% V)	6.9×10^{-5}	5.75×10^{-5}

where it rapidly vaporized. The gaseous mixture of acetaldehyde and air inside the reactor was constantly magnetically stirred. Before analysis, the catalyst and acetaldehyde were kept in the reactor for about 30 min to obtain a uniform gas-phase concentration. The reactor was cooled by water circulation, and the experiments were performed at 25 °C. Gaseous samples (35 μL) were periodically (every 10 min) extracted from the reactor and analyzed by GCMS [gas chromatograph equipped with a mass selective detector (Shimadzu GCMS-QP5000)]. The temperatures of the column, injector, and detector were maintained at 40, 200, and 280 °C, respectively.

3. Results and discussion

The evolution of CO_2 during acetaldehyde degradation was used to estimate the activity of the catalysts. The activity also was measured for 40 min before the light source was activated. Fig. 1 shows the CO_2 evolution on different catalysts. The photocatalytic activity of doped TiO_2 was greatly enhanced by incorporating it with carbon and vanadium. Most importantly, the carbon and vanadium co-doped TiO_2 demonstrated high activity in the dark; the higher values at zero time were due to reaction in the dark occurring during the 30 min before sampling. To enable quantitative comparison, the initial rates for the initial 40 min (with or without irradiation) are calculated to represent the activities. These values are shown in Table 1. In the dark, P25 TiO_2 and C-doped TiO_2 showed no activity;

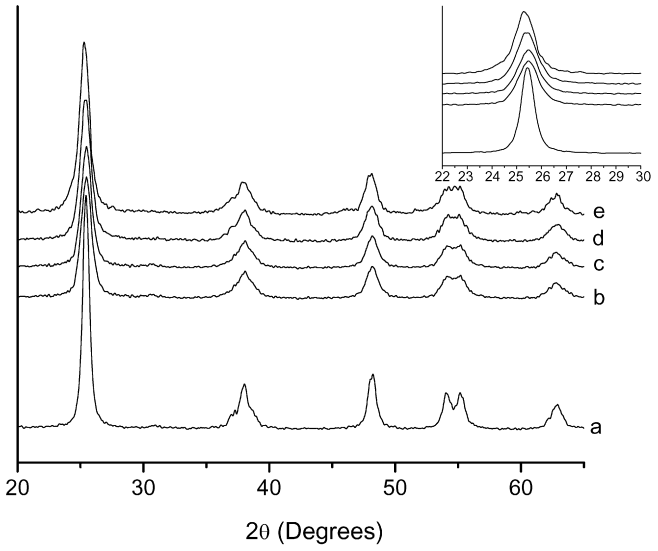

Fig. 2. X-ray diffraction patterns of un-doped and doped TiO_2: (a) un-doped TiO_2, (b) co-doped TiO_2, (c) C-doped TiO_2 (0.5% V), (d) co-doped TiO_2 (2.0% V), (e) co-doped TiO_2 (3.0% V).

however, with the addition of vanadium, the co-doped TiO_2 catalysts were highly active for the degradation of acetaldehyde, especially when the vanadium loading was 2%. Under visible irradiation, the photocatalytic reactivity of C-doped TiO_2 was 8.2 times greater than that of P25 TiO_2, and that of co-doped TiO_2 was 6.6 times higher, for a 2.0% loading; a 3.0% loading was less effective. Moreover, for co-doped TiO_2 with 2% vanadium content, the activity was comparable in the dark and under visible irradiation. The different activities among these catalysts likely result from different physical properties and reaction mechanisms, as discussed later.

Fig. 2 shows the XRD patterns of pure TiO_2 and doped TiO_2. TiO_2 anatase diffraction lines can be seen in all XRD patterns; no other crystal phase (rutile or brookite) can be detected. The strongest peak at $2\theta = 25.3°$ is representative of (101) anatase-phase reflections. The inset of Fig. 2 is an enlargement of the (101) plane of all of these samples. Compared with pure TiO_2, the peak position of the (101) plane of C-doped TiO_2 shifted slightly to a higher 2θ value, and the peak was broader, suggesting distortion of the crystal lattice of doped TiO_2 by the incorporation of elemental carbon and smaller particle size of the C-doped TiO_2. Greater distortion of the structures occurred with the addition of vanadium, indicating that vanadium (V^{4+}) was incorporated into the lattice and substituted for Ti^{4+}, as suggested by the XPS spectra (see later discussion).

From the full width at half maximum (FWHM) of the diffraction pattern, the particle sizes were calculated using Scherrer's equation. Pure TiO_2 had a particle size of 14 nm; doped TiO_2, about 9 nm (see Table 2). No diffraction lines due to TiC, TiN, and TiS were found, consistent with the XPS results discussed later. Furthermore, no separate VO_x phases were observed for any of the vanadium-containing samples, possibly due to the high dispersion or the very small crystallite size of vanadia species that may be present.

Table 2
Surface area and particle size of samples

Sample	Surface area[a] (m^2/g)	Particle size[b] (nm)
TiO_2	57	14.0
C-doped TiO_2	98	8.9
C-, V-doped TiO_2 (0.5% V)	96	8.9
C-, V-doped TiO_2 (1.0% V)	94	9.0
C-, V-doped TiO_2 (2.0% V)	94	9.2
C-, V-doped TiO_2 (3.0% V)	59	10.3

[a] By BET.
[b] By XRD.

To investigate the chemical states of the possible dopants incorporated into TiO_2, Ti 2p, C 1s, S $2p_{3/2}$, N 1s, and V $2p_{3/2}$ binding energies were studied by measuring the XPS spectra. The results are shown in Fig. 3.

Two peaks for the Ti 2p XPS spectrum were observed at 464.2 and 458.5 eV, assigned to Ti $2p_{1/2}$ and $2p_{3/2}$, respectively. These values agree well with XPS data in the literature and are known to be due to Ti^{4+} in pure anatase titania form [12].

The C 1s XPS spectrum showed one peak at 284.8 eV and a shoulder at around 288.6 eV. The feature at 284.8 eV can be assigned to elemental carbon, and the shoulder around 288.6 eV suggests the existence of carbonate species [15,16]. After sputtering, the shoulder at around 288.6 eV disappeared, indicating that carbonate species existed only on the surface. The peak at 284.8 eV remained, and the intensity decreased only slightly. These results strongly imply elemental carbon deposits not only on the surface, but also in the bulk of the TiO_2 powder. A peak around 281 eV, reportedly resulting from the Ti–C bond [22], was not observed in our sample.

The S $2p_{3/2}$ XPS spectrum showed a peak at around 168.3 eV. A broad peak attributed to S $2p_{3/2}$ at around 168 eV was reported to consist of several oxidation states of S atoms. The peak of the S^{6+} state appeared at 168.2 eV by studying the XPS spectra of pure TiO_2 immersed in H_2SO_4 aqueous solution followed by calcination at 500 °C for 3 h, and the peak at 167.5 eV was assigned to S^{4+} [16,23]. Sayago et al. [24] reported that the peak of the S 2p state was in the region of 166–170 eV for adsorbed SO_2 molecules on a TiO_2 surface. Because our samples were calcined in air at 500 °C, the S $2p_{3/2}$ peak can be attributed to the S^{6+} state. The S 2p peak at 160–163 eV, coming from S atoms substituting for O atoms on the TiO_2 surface [25], was not observed in our case. The disappearance of the S $2p_{3/2}$ peak after sputtering indicates that sulfur species appeared only on the surface. The formation of carbonate (1448 cm^{-1}) and sulfate species (1100 cm^{-1}) is supported by the FTIR spectra displaying their characteristic band structures (not shown here).

The N 1s XPS spectrum exhibited a peak at around 399 eV. The value is consistent with XPS data from chemisorbed N_2 molecules [26] or molecularly adsorbed N-containing compounds (NO_x and NH_3, which formed during the decomposition and oxidation of the N precursors) [27]. The feature at around 396 eV, generally assigned to N^{2-} anions resulting from substitution for oxygen sites by nitrogen atoms in the TiO_2 lattice [26,28,29], was not observed. Based on our preparation process, the peak around 399 eV can be assigned to adsorbed NO_x or NH_3. Clearly, however, these nitrogen species also exist only on the surface of TiO_2, as demonstrated by the disappearance of the peak after sputtering.

The O 1s satellite obviously interfered with the V $2p_{3/2}$ XPS peak. The magnitude of the V $2p_{3/2}$ peak was small, and the peak appeared as two shoulders. The shoulder at a binding energy of 516.9 eV suggests V^{5+} species, whereas the shoulder at 516.3 eV can be assigned to V^{4+}. These values are consistent with a binding energy of V $2p_{3/2}$ measured for the V_2O_5/TiO_2 catalyst [30,31]. V^{4+} ions were incorporated into the crystal lattice of TiO_2 and no vanadium–titanium phase was present; thus, V^{4+} ions substituted for Ti^{4+} ions and formed a Ti–O–V bond. Obviously, some V^{4+} ions were oxidized into V^{5+} in the preparation process, because vanadium existed only as V^{4+} in the precursor; the formation of V^{5+} possibly occurred during annealing.

Fig. 4 shows the UV–vis absorption spectra of the un-doped and doped TiO_2. Commercial Degussa P-25 TiO_2 exhibited absorption only in the UV region. The onset absorption spectrum of pure TiO_2 showed a very weak red shift; however, significant photoabsorption was demonstrated in the visible region of the doped TiO_2. The C-doped TiO_2 absorbed the photoenergy in the visible region up to 600 nm, indicating that the incorporated elemental carbon was acting as a photosensitizer [17]. With the addition of vanadium, the absorption curve of the co-doped TiO_2 extended to 800 nm. It has been reported that V^{5+} shows an absorption at <570 nm and that V^{4+} has an absorption band centered at 770 nm [32], therefore, the spectra suggest the co-existence of V^{5+} and V^{4+}, consistent with the XPS spectra. The tailing of the absorption band can be assigned to the charge-transfer transition from the d orbital of V^{4+} to the conduction band of TiO_2 [33]. In the presence of visible light, this photoexcited electron apparently enabled chemical reactions at the surface of V-doped TiO_2, because the oxidation of V^{4+} to V^{5+} occurred 2.1 eV below the TiO_2 conduction band [34]. The extended visible absorption obviously suggested modified electronic properties from the incorporation of vanadium, forming impurity energy levels between the valence band and conduction band of TiO_2 [7].

3.1. Mechanistic studies

Fig. 1 illustrates that P25 TiO_2 and C-doped TiO_2 were inactive in the dark for the degradation of acetaldehyde. With the introduction of vanadium, modified TiO_2 showed high activity in the dark. XRD spectra indicated no new vanadium–titanium compound; thus the increase in the activity must be due to a change in the surface of the catalyst resulting from vanadium substitution.

Based on the characterization results, the following explanation for the high activity in the dark can be considered. During catalyst preparation, V^{4+} ions are incorporated into the bulk and on the surface of TiO_2 in the gelation stage. It is possible that V^{4+} in the sublayers of TiO_2 is oxidized to V^{5+} during

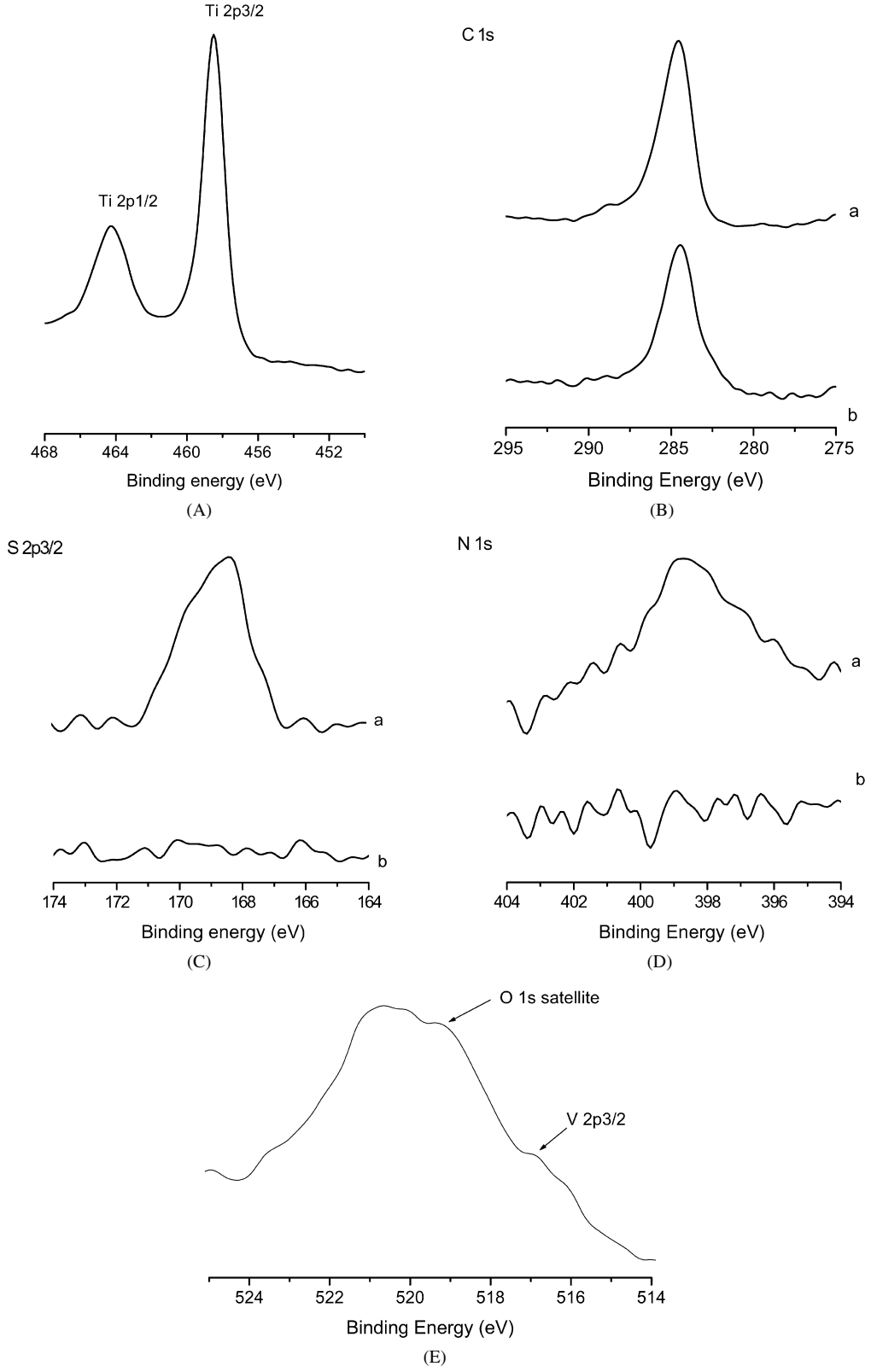

Fig. 3. XPS spectra of C-doped TiO_2: (A) Ti 2p, (B) C 1s, (C) S $2p_{3/2}$, (D) N 1s ((a) before sputtering; (b) after sputtering) and C-, V-doped TiO_2 (2.0% V): (E) V $2p_{3/2}$.

water removal and/or calcination in air. If pentavalent V^{5+} ions are present at tetravalent sites (Ti^{4+} or V^{4+}), then the substitution could induce a free electron [35]. V^{5+} ion shares only four valence electrons with four O^{2-} neighbor ions. The fifth electron cannot be shared and is delocalized around the V^{5+} positive center. Only a small amount of thermal energy is needed to delocalize this electron and promote it into the conduction band [35]. In the dark, the promoted electron can be transferred

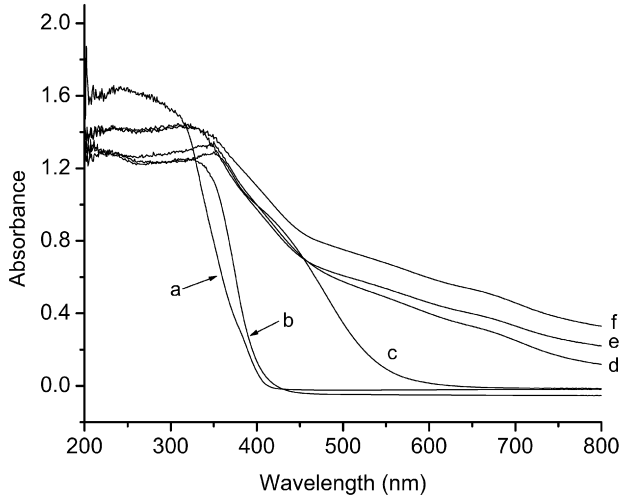

Fig. 4. Diffuse reflectance spectra of P25 TiO_2, un-doped and doped TiO_2: (a) P25, (b) TiO_2, (c) C-doped TiO_2, (d) C-, V-doped TiO_2 (0.5% V), (e) C-, V-doped TiO_2 (2.0% V), (f) C-, V-doped TiO_2 (3.0% V).

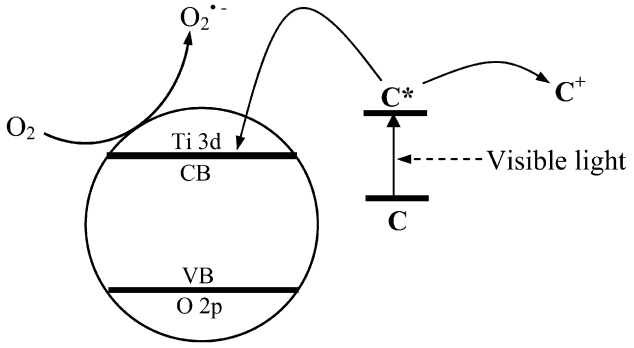

Scheme 1. Proposed electron transfer pathway to produce superoxide radical anion, $O_2^{\bullet-}$, on C-doped TiO_2 particles under visible light irradiation (C refers to elemental carbon).

to triplet oxygen to generate the superoxide radical anion $O_2^{\bullet-}$, which is known to degrade organic compounds [17,36]. When the loading of vanadium increases from 0.5 to 2.0%, more V^{4+} ions in the sublayer of TiO_2 are possibly oxidized into V^{5+}, enhancing the activity. But further increasing the vanadium content could deteriorate the dispersion and lead to the aggregation of vanadium, as indicated by the smaller surface area; that is why, as shown in Fig. 1, the activity decreased when the vanadium loading increased from 2.0 to 3.0%.

Under visible light irradiation, two major reaction pathways can be considered:

1. The elemental carbon acts as a photosensitizer. As shown in Scheme 1, in the presence of visible light, the excited photosensitizer injects an electron into the conduction band of titanium dioxide. Subsequently, the electron is transferred to oxygen adsorbed on the TiO_2 surface, producing $O_2^{\bullet-}$, which is capable of degrading organic compounds [17]. After a series of reactions, acetaldehyde molecules are finally degraded into CO_2 and H_2O.
2. The incorporation of vanadium into the crystal lattice of TiO_2 modifies the electronic properties of TiO_2. Because the oxidation V^{4+} to V^{5+} occurs at 2.1 eV below the TiO_2 conduction band, a 3d electron from a V^{4+} center is readily photoexcited into the TiO_2 conduction band under visible light irradiation [34], generating $O_2^{\bullet-}$ similarly to the mechanism shown in pathway 1. It is assumed that this photoexcited electron initiates chemical reactions [10].

For C-doped TiO_2, pathway 1 is involved in the photoreaction. Both pathways are included for C- and V-co-doped TiO_2. Compared with the transition metal loading level in the range of 0.1–0.5% for the enhancement of TiO_2 photoreactivity [33], our samples have a much higher vanadium content. As shown in Table 2, the effective samples have much higher surface areas; therefore, along with its function as a photosensitizer, the doped elemental carbon also increases the surface area, which significantly increases the dispersion of vanadium and may provide more possibly accessible active sites, enhancing activity. In addition, high surface areas are beneficial for the sorption of acetaldehyde on the catalyst surface. The decreased activity for the co-doped TiO_2 with an increase in vanadium loading from 2 to 3% may be due to poor dispersion, reduced surface area, and aggregation of vanadium, such as V_2O_5. Pure V_2O_5 and TiO_2-supported V_2O_5 that fail to enter the structure of the solid solution do not show any photocatalytic activity [4].

4. Conclusion

C-doped and C- and V-co-doped TiO_2 catalysts were successfully synthesized by a sol–gel process. The C-doped TiO_2 showed high activity for the degradation of acetaldehyde under visible irradiation. The doped elemental carbon acted as a photosensitizer and increased the surface area, resulting in high dispersion of vanadium for the co-doped TiO_2 catalysts, which showed high activity both in the dark and under visible light irradiation. The insertion of pentavalent V^{5+} into tetravalent sites induced a free electron that could be delocalized and promoted into the conduction band of TiO_2 by only slight thermal energy. The superoxide radical anion $O_2^{\bullet-}$, produced when the free electron was transferred to adsorbed O_2, was responsible for the degradation of acetaldehyde. We report here for the first time that the activities were comparable in the dark and under visible light irradiation for the co-doped TiO_2, especially when at a vanadium content of 2.0%. Under visible light irradiation, the incorporation of vanadium introduced impurity levels between the valence and conduction band of TiO_2, allowing ready photoexcitation of electrons into the conduction band, initiating the chemical reaction.

Acknowledgments

This work was supported by the Army Research Office and Kansas State University Targeted Excellence Program.

References

[1] M.A. Fox, M.T. Dulay, Chem. Rev. 93 (1993) 341.
[2] A.L. Linsebigler, G. Lu, J.T. Yates Jr., Chem. Rev. 95 (1995) 735.

[3] J.H. Carey, J. Lawrence, H.M. Tosine, Bull. Environ. Contam. Toxicol. 16 (1976) 697.
[4] J.C. Yu, J. Lin, R.W.M. Kwok, J. Photochem. Photobiol. A Chem. 111 (1997) 199.
[5] C. Burda, Y. Lou, X. Chen, A.C.S. Samia, J. Stout, J. Gole, Nano Lett. 3 (2003) 1049.
[6] X. Li, F. Li, C. Yang, W. Ge, J. Photochem. Photobiol. A Chem. 141 (2001) 209.
[7] M. Anpo, S. Dohshi, M. Kitano, Y. Hu, M. Takeuchi, M. Matsuoke, Annu. Rev. Mater. Res. 35 (2005) 1.
[8] S. Yin, H. Yamaki, M. Komatsu, Q. Zhang, J. Wang, Q. Tang, F. Saito, T. Sato, J. Mater. Chem. 13 (2003) 2996.
[9] H. Irie, Y. Wanatabe, K. Hashimoto, J. Phys. Chem. B 107 (2003) 5483.
[10] S. Klosek, D. Raftery, J. Phys. Chem. B 105 (2001) 2815.
[11] J.C.S. Wu, C.H. Chen, J. Photochem. Photobiol. A Chem. 163 (2004) 509.
[12] S. Joung, T. Amemiya, M. Murabayashi, K. Itoh, Chem. Eur. J. 12 (2006) 5526.
[13] T. Umebayashi, T. Yamake, H. Itoh, K. Asai, Appl. Phys. Lett. 81 (2002) 454.
[14] T. Ohno, T. Mitsui, M. Matsumura, Chem. Lett. 32 (2003) 364.
[15] S. Sakthivel, H. Kisch, Angew. Chem. Int. Ed. 42 (2003) 4908.
[16] T. Ohno, T. Tsubota, K. Nishijima, Z. Miyamoto, Chem. Lett. 33 (2004) 750.
[17] C. Lettmann, K. Hildenbrand, H. Kisch, W. Macyk, W. Maier, Appl. Catal. B Environ. 32 (2001) 215.
[18] H. Sun, Y. Bai, Y. Cheng, W. Jin, N. Xu, Ind. Eng. Chem. Res. 45 (2006) 4971.
[19] W. Zhao, W. Ma, C. Chen, J. Zhao, Z. Shuai, J. Am. Chem. Soc. 126 (2004) 4782.
[20] H. Wei, Y. Wu, N. Lun, F. Zhao, J. Mater. Sci. 39 (2004) 1305.
[21] Y. Sakatani, J. Nunoshige, H. Ando, K. Okusako, H. Koike, T. Takata, J.N. Kondo, M. Hara, K. Domen, Chem. Lett. 32 (2003) 1156.
[22] H. Irie, Y. Watanabe, K. Hashimoto, Chem. Lett. 32 (2003) 772.
[23] T. Ohno, Water Sci. Technol. 49 (2004) 159.
[24] D.I. Sayago, P. Serrano, O. Bohme, A. Goldoni, G. Paolucci, E. Roman, J.A. Martin-Gago, Phys. Rev. B 64 (2001) 205402.
[25] E.L.D. Hebenstreit, W. Hebenstreit, U. Diebold, Surf. Sci. 470 (2001) 347.
[26] N.C. Saha, H.G. Tompkins, J. Appl. Phys. 72 (1992) 3072.
[27] D. Li, N. Ohashi, S. Hishita, T. Kolodiazhnyi, H. Handea, J. Solid State Chem. 178 (2005) 3293.
[28] H. Irie, Y. Watanabe, K. Hashimoto, J. Phys. Chem. B 107 (2003) 5483.
[29] O. Diwald, T.L. Thompson, T. Zubkov, E.G. Goralski, S.D. Walck, J.T. Yates, J. Phys. Chem. B 108 (2004) 6004.
[30] M. Kobayashi, R. Kuma, S. Masaki, N. Sugishima, Appl. Catal. B Environ. 60 (2005) 173.
[31] S.L.T. Andersson, Catal. Lett. 7 (1990) 351.
[32] H. Ozaki, S. Iwamoto, M. Inoue, Catal. Lett. 113 (2007) 95.
[33] W. Choi, A. Termin, M.R. Hoffmann, J. Phys. Chem. 98 (1994) 13669.
[34] K. Mizushima, M. Tanaka, A. Asai, S. Iida, J.B. Goodenough, J. Phys. Chem. Solids 40 (1979) 1129.
[35] J.M. Herrmann, J. Disdier, G. Deo, I.E. Wachs, J. Chem. Soc. Faraday Trans. 93 (1997) 1655.
[36] M.M. Mohamed, M.M. Al-Esaimi, J. Mol. Catal. A Chem. 255 (2006) 53.